

Thick-Film Structure Geometry Effect on Carbon Nanotubes Synthesized by Chemical Vapor Deposition

This content has been downloaded from IOPscience. Please scroll down to see the full text.

2008 Jpn. J. Appl. Phys. 47 4788

(<http://iopscience.iop.org/1347-4065/47/6R/4788>)

View [the table of contents for this issue](#), or go to the [journal homepage](#) for more

Download details:

IP Address: 140.113.38.11

This content was downloaded on 25/04/2014 at 16:07

Please note that [terms and conditions apply](#).

Thick-Film Structure Geometry Effect on Carbon Nanotubes Synthesized by Chemical Vapor Deposition

Kuang-Chung CHEN¹, Chia-Fu CHEN^{1,2*}, Wha-Tzong WHANG¹, Shu-Hsing LEE³, Kuo-Feng CHEN³, Chian-Liang HWANG⁴, Nyan-Hwa TAI⁴, Ming-Hung LIN³, and Lih-Hsiung CHAN³

¹Department of Materials Science and Engineering, National Chiao Tung University, Hsinchu, Taiwan 300, R.O.C.

²Institute of Material and System Engineering, MingDao University, Changhua, Taiwan 52345, R.O.C.

³Display Technology Center (DTC), Industrial Technology Research Institute (ITRI), Hsinchu, Taiwan 310, R.O.C.

⁴Department of Materials Science and Engineering, National Tsing Hua University, Hsinchu, Taiwan 300, R.O.C.

(Received September 26, 2007; accepted February 17, 2008; published online June 13, 2008)

In chemical vapor deposition (CVD) technology, the mass flow transport behaviors of precursor gases play an important role particularly in thick-film normal triode structures. The depth dimension of dielectric holes in thick-film normal triode structures may range from 10 to 50 μm . The relationship between carbon nanotube (CNT) synthesis and aspect ratio of dielectric holes is investigated in this work. In high-aspect-ratio dielectric holes (such as narrow and deep holes), precursor diffusion driven by concentration gradient must be combined with pumping assistance in order to force reactive gas to flow toward the catalyst at the bottom of dielectric holes for CNT growth. [DOI: 10.1143/JJAP.47.4788]

KEYWORDS: CVD, carbon nanotubes, thick-film structure

1. Introduction

The discovery of carbon nanotubes (CNTs) by Iijima in 1991 resulted in a new scientific research field in both academe and industry.¹⁾ CNTs have aroused considerable attention owing to their unique properties, such as high mechanical strength, high chemical stability, and high aspect ratio for field emission applications.^{2–6)} Recently, chemical-vapor-deposited CNTs and arc-discharge-produced and pulsed-laser-ablation-produced CNTs have been reported to exhibit excellent field emission characteristics such as low turn-on voltage and high current density.^{7–9)} Among the above methods, both arc discharge and chemical vapor deposition (CVD) were often reported to be used for field emission display.^{10,11)} A low-cost process combining arc-discharge-produced CNTs and screen-printing technologies was developed to prepare field emitters on glass substrates.^{12,13)} Unfortunately, using CNT paste in the screen-printing technology results in relatively low resolution and requires a surface rubbing technology or other activation steps to enhance the field emission characteristics.¹²⁾ On the other hand, CVD can be used to directly grow CNTs on a predefined catalyst layer and has high yield and uniformity without activation methods.¹⁴⁾

Many researchers have succeeded in synthesizing CNTs on Si substrate at a relatively high temperature by various CVD methods.^{15,16)} To suit field emission display (FED) applications, the growth temperature should be below 550 °C to avoid glass substrate deformation. Consequently, the direct growth of CNTs at low temperature on glass substrates by CVD methods has been reported.^{17–19)} However, in previous studies, it was necessary to construct the triode structure on glass substrates by semiconductor processes, such as sputtering, thermal evaporation, or CVD methods. It is well-known that the semiconductor processes are much more expensive than screen-printing processes. Therefore, the direct growth of CNTs in the triode structure at low temperature by a low-cost technology will play an important role in practical FED applications. To achieve these require-

ments, our work was to combine the thick-film screen-printing and photolithography technologies to construct the triode electronic structure, in which CNTs were then synthesized in the selected area by CVD. By controlling the pumping system and precursor concentration during the CVD, the cathode for field emission devices was properly produced.

2. Experiments

2.1 Structure construction

To investigate the structure geometric effects on the CVD CNT process, we constructed three different types of structure with different morphologies. The conductive electrodes in the three structures were all screen-printed with silver paste and patterned by photolithography methods. The organic solvents were removed by the following 400 °C firing process, and then glass frits were sintered at 550 °C for 15 min.

The first type (type A) structure was the planar electrode structure, as seen in Fig. 1(a). The width and thickness of the cathode electrode were ~ 300 and ~ 10 μm , respectively. A catalyst was selectively deposited on these patterned electrodes with the aid of a photoresist. In the type B structure [Fig. 1(b)], we printed and patterned a trench-morphology-structured dielectric layer on the conductive electrode. The depth of the trench was ~ 15 μm , while the open width was ~ 180 μm . A catalyst was coated on both the dielectric layer and conductive electrode in order to trace the difference in these two positions (on the top area and at the bottom of the trench structure).

Type C was a conventional normal triode structure [Fig. 1(c)]. The pixel size was $\sim 350 \times \sim 110$ μm^2 , with a depth of ~ 15 μm . The type C structure showed a smaller open-sized and deeper hole morphology, compared with those of types A and B. A catalyst was selectively deposited on the cathode electrode at the bottom of the dielectric hole. Types A to C were observed by scanning electron microscopy (SEM), and shown in Figs. 2(a)–2(c), respectively.

2.2 CVD

The samples were loaded into a thermal CVD chamber and heated to a synthesis temperature of 500 °C. The

*E-mail address: cfchen@mdu.edu.tw

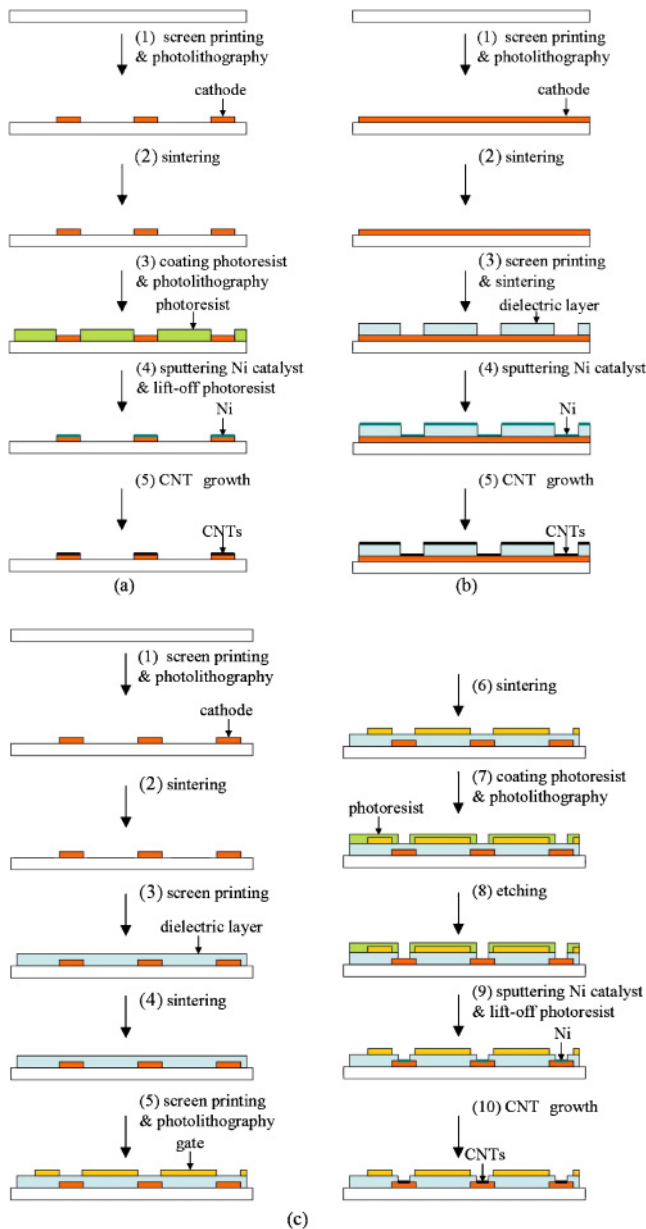


Fig. 1. (Color online) Schematic illustrations of (a) type A, (b) type B, and (c) type C structure fabrication processes.

reduction step was carried out under 600 sccm H_2 atmosphere for 10 min, followed by the CNT growth step under 300 sccm H_2 and 300 sccm acetylene (C_2H_2) atmospheres for 15 min. The structures and morphologies of CNTs were observed by SEM (Hitachi S-4000) and optical microscope (OM).

3. Results and Discussion

In type A, precursor gases loaded into the chamber are able to react with the catalyst coated on the conductive electrode without any difficulty. Carbon atoms can move from the gas phase to the catalyst metal, supersaturate in the catalyst, and then precipitate to form CNTs (as shown in Fig. 3). There is no obstacle that can restrict or affect the gas flow behavior.

Then, we built the environment of “side walls” surrounding the conductive electrodes, as shown in type B. The goal is to investigate whether such trench morphology can play an important role in affecting the gas flow. Results show that CNTs can be synthesized both “on the top of the trench

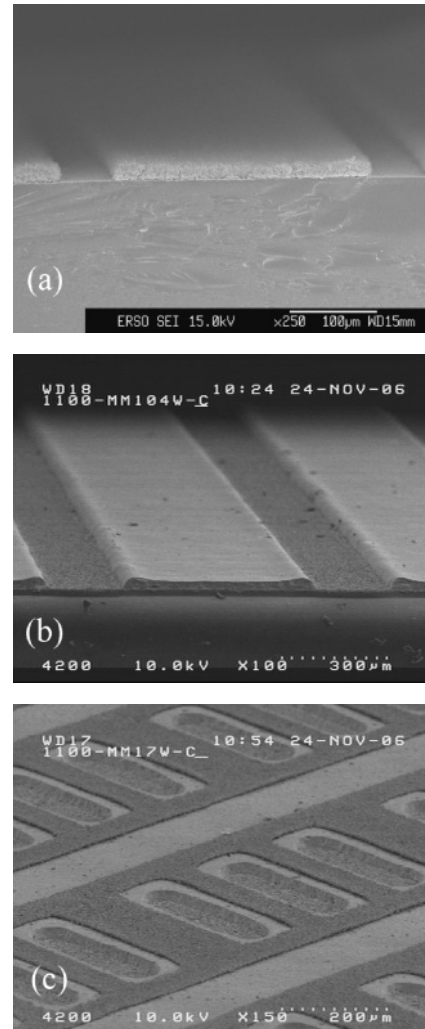


Fig. 2. SEM images of cross-sectional view of (a) type A, (b) type B, and (c) type C structures.

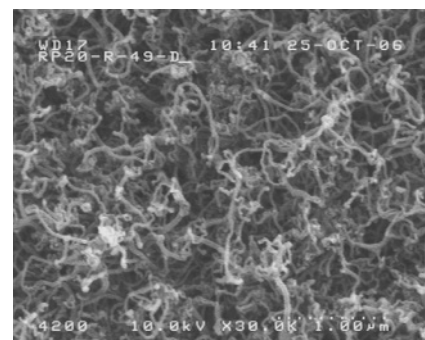
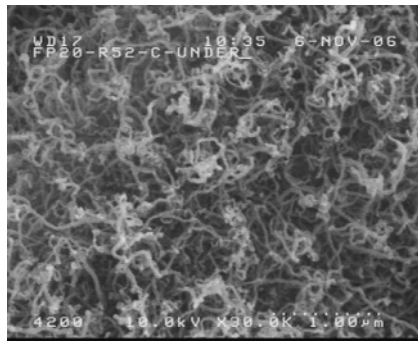


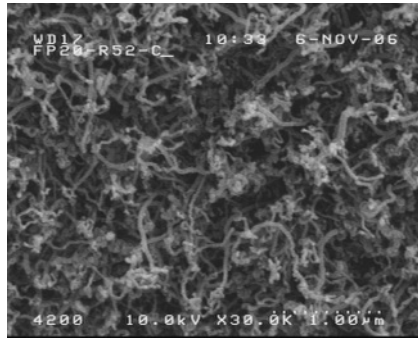
Fig. 3. SEM image of surface morphology of CNTs grown at 500 °C for 15 min with 300 sccm C_2H_2 and 300 sccm H_2 .

structure” and “at the bottom of the trench structure”, as shown in Figs. 4(a) and 4(b), respectively. The morphologies of the CNTs at these two different positions are similar without any obvious difference. It was implied that the depth of the trench structure and the aspect ratio of the trench cannot affect the CNT growth. The gas flow and transport path are still unobstructed inside the trench.

In practical FED devices, the matrix of the pixels is fabricated in the cathode plate. The CNT emitters are located



(a)



(b)

Fig. 4. SEM images of surface morphology of CNTs grown (a) at the bottom and (b) on the top area of the trench structure at 500°C for 15 min with 300 sccm C₂H₂ and 300 sccm H₂.

at the bottom of the dielectric holes, while the gate electrodes over the CNT emitters serve as driving electrodes. For high-resolution display application, the pixel size is reduced to a much smaller scale. Thus, dielectric holes become much more narrow and deeper. In the type C structure, such holes perform a morphology in which gas flow and transport are no longer smooth. Figure 5 shows that only amorphous carbon particles are synthesized at the bottom of dielectric holes under the same growth recipes as those in the types A and B structures. Although different ratios of precursor gases are tested, we still obtain the same results. It implies that the problem originating from hole geometry morphology cannot be solved by merely changing the precursor ratios. If the original atmosphere existing inside the dielectric holes cannot exchange with active precursor gases, the decomposed carbon atoms can move toward the catalyst only by being driven by the concentration gradient. The precursor gases might form a steady flowing state just over the dielectric holes (but not flow into and then out of the holes). The amount of carbon atoms driven only by the concentration gradient is not sufficient for the supersaturation and precipitation reaction. Thus, only carbon particles are coated at the bottom of the dielectric holes.

Such phenomenon cannot appear in the normal triode structure fabricated by fully thin-film processes.¹⁸⁾ The depth of the dielectric holes in the thin-film processes is often no more than 1 μm. The effect resulting from the depth of such dielectric holes is not obvious in terms of the flow behavior of precursor gases. However, in the thick-film processes, it does play an important role in the synthesis of CNTs.

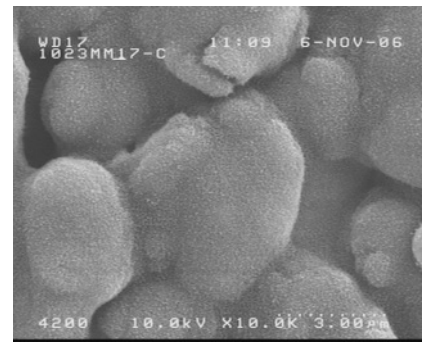


Fig. 5. SEM image of surface morphology of CNTs grown at the bottom of the dielectric hole at 500°C for 15 min with 300 sccm C₂H₂ and 300 sccm H₂ without pumping assistance.

Table I. Summary of pumping process effects on CNT growth.

Step 1 (reduction)	Step 2 (growth)	Result
Hydrogen pumping	Acetylene pumping	CNTs
	Without acetylene pumping	No CNTs
Without hydrogen pumping	Acetylene pumping	CNTs
	Without acetylene pumping	No CNTs

To solve this problem, we adopt the pumping procedure before the hydrogen reduction step and before the CNT growth step. The background pressure is pumped to 460 Torr, and then hydrogen gas is fed into the chamber to activate the catalyst under 600 Torr background pressure. After the activation step, another pumping proceeds to maintain the background pressure at 460 Torr again. In the following step, a mixture of hydrogen and acetylene is loaded to grow the CNTs. Pumping assistance can help drive the original existing gas out of the dielectric holes and force precursor gases to flow into the holes. We have tested several different growth conditions with or without the pumping processes during the reduction and growth steps, the results of which are listed in Table I. It was found that no carbon nanotubes were observed without acetylene pumping, whether hydrogen atmosphere was under pumping or not. Therefore, we conclude that the floating behavior of the carbon source atmosphere plays an important role. Thus, we adopt the pumping procedure during the reduction and growth steps to simplify the processes. Figure 6(a) shows the cathode plate after growth under optical microscopy observation, while Fig. 6(b) shows the CNT growth results at the bottom of the dielectric hole under SEM observation. The difference between the left-hand and the right-hand parts of Fig. 6(a) was catalyst deposition. The catalyst was selectively deposited on the left-hand part of the cathode electrode in accordance with the photoresist definition. The left-hand part of Fig. 6(a) shows the CNT selective growth on the cathode electrode with the catalyst deposited, but the right-hand part of Fig. 6(a) shows a clear cathode electrode without the catalyst deposited under the same growth condition. The density of the CNTs is approximately 10⁶ CNTs/cm², which is still lower than those in Figs. 4(a) and 4(b).

4. Conclusions

In this work, we have demonstrated that precursor gas

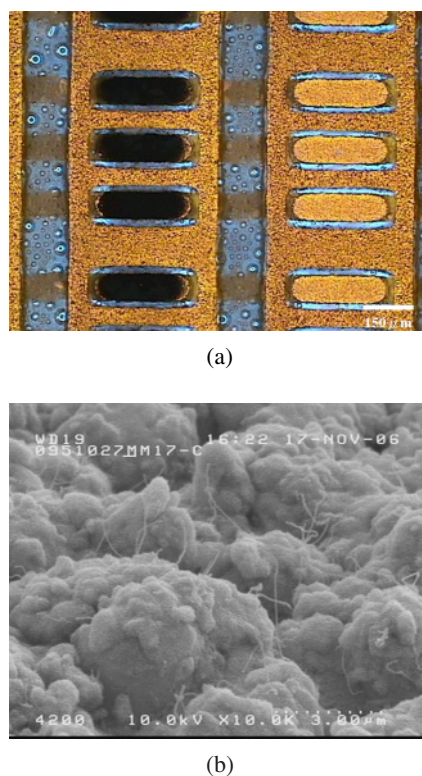


Fig. 6. (Color online) (a) OM image and (b) SEM image of CNTs grown at the bottom of the dielectric hole at 500°C for 15 min with 300 sccm C_2H_2 and 300 sccm H_2 at 600 Torr with pumping assistance. (The left-hand part of (a) shows the CNT selective growth on the cathode electrode with the catalyst deposited, but the right-hand part of (a) shows a clear cathode electrode without the catalyst deposited.)

flow and transport are unobstructed in both planar electrode and trench morphology structures. Regarding the thick-film normal triode structure, additional pumping assistance is

required in order to solve the gas transport problem in such narrow and deep dielectric holes.

- 1) S. Iijima: *Nature* **354** (1991) 56.
- 2) W. A. de Heer, A. Chatelain, and D. Ugarte: *Science* **270** (1995) 1179.
- 3) S. Fan, M. G. Chapline, N. F. Franklin, T. W. Tomblor, A. M. Cassel, and H. Dai: *Science* **283** (1999) 512.
- 4) K. A. Dean and B. R. Chalamala: *Appl. Phys. Lett.* **75** (1999) 3017.
- 5) P. G. Collins and A. Zettl: *Appl. Phys. Lett.* **69** (1996) 1969.
- 6) Q. H. Wang, A. A. Setlur, J. M. Lauerhass, J. Y. Dai, E. W. Seeling, and R. P. H. Chang: *Appl. Phys. Lett.* **72** (1998) 2912.
- 7) P. M. Ajayan and S. Iijima: *Nature* **361** (1993) 333.
- 8) Z. W. Pan, S. S. Xie, B. H. Chang, L. F. Sun, W. Y. Zhou, and G. Wang: *Chem. Phys. Lett.* **299** (1999) 97.
- 9) S. Bandow, A. M. Rao, K. A. Williams, A. Thess, R. E. Smalley, and P. C. Eklund: *J. Phys. Chem. B* **101** (1997) 8839.
- 10) P. G. Collins and A. Zettl: *Phys. Rev. B* **55** (1997) 9391.
- 11) Y. Chen, D. T. Shaw, and L. Guo: *Appl. Phys. Lett.* **76** (2000) 2469.
- 12) W. B. Choi, D. S. Chung, J. H. Kang, H. Y. Kim, Y. W. Jin, I. T. Han, Y. H. Lee, J. E. Jung, N. S. Lee, G. S. Park, and J. M. Kim: *Appl. Phys. Lett.* **75** (1999) 3129.
- 13) J. E. Jung, Y. W. Jin, J. H. Choi, Y. J. Park, T. Y. Ko, D. S. Chung, J. W. Kim, J. E. Jang, S. N. Cha, W. K. Yi, S. H. Cho, M. J. Toon, C. G. Lee, J. H. You, N. S. Lee, J. B. Yoo, and J. M. Kim: *Physica B* **323** (2002) 71.
- 14) K. C. Chen, C. F. Chen, J. S. Chiang, C. L. Hwang, Y. Y. Chang, and C. C. Lee: *Thin Solid Films* **498** (2006) 198.
- 15) G. S. Choi, Y. S. Cho, S. Y. Hong, J. B. Park, K. H. Son, and D. J. Kim: *J. Appl. Phys.* **91** (2002) 3847.
- 16) V. K. Kayastha, Y. K. Yap, Z. Pan, I. N. Ivanov, A. A. Puzetzy, and D. B. Geohegan: *Appl. Phys. Lett.* **86** (2005) 253105.
- 17) H. S. Kang, H. J. Yoon, C. O. Kim, J. P. Hong, I. T. Han, S. N. Cha, B. K. Song, J. E. Jung, N. S. Lee, and J. M. Kim: *Chem. Phys. Lett.* **349** (2001) 196.
- 18) J.-H. Han, S. H. Choi, T. Y. Lee, J.-B. Yoo, C.-Y. Park, H. J. Kim, I.-T. Han, S. Yu, W. Yi, G. S. Park, M. Yang, N. S. Lee, and J. M. Kim: *Thin Solid Films* **409** (2002) 126.
- 19) C. J. Lee, J. Park, S. Han, and J. Ihm: *Chem. Phys. Lett.* **337** (2001) 398.
- 20) Y.-M. Shyu and F. C.-N. Hong: *Mater. Chem. Phys.* **72** (2001) 223.